International Journal of Non-Linear Mechanics 43 (2008) 551 – 561

Contents lists available at ScienceDirect

International Journal of Non-Linear Mechanics

journal homepage: www.elsevier.com/locate/nlm

Non-linear modal analysis for beams subjected to axial loads: Analytical and finite-element solutions

Carlos E.N. Mazzilli[a,*], César T. Sanches[a], Odulpho G.P. Baracho Neto[a], Marian Wiercigroch[b], Marko Keber[b]

[a]Department of Structural and Geotechnical Engineering, University of São Paulo, Av. Prof. Almeida Prado, trav.2 n. 83, São Paulo 05508-900, Brazil
[b]Centre for Applied Dynamics Research, School of Engineering, University of Aberdeen, Kings College, Aberdeen AB24 3UE, UK

ARTICLE INFO

Article history:
Received 12 April 2007
Received in revised form 27 March 2008
Accepted 6 April 2008

Keywords:
Non-linear normal modes
Non-linear multi-modes
Axially loaded beams
Vertical risers

ABSTRACT

A rigorous derivation of non-linear equations governing the dynamics of an axially loaded beam is given with a clear focus to develop robust low-dimensional models. Two important loading scenarios were considered, where a structure is subjected to a uniformly distributed axial and a thrust force. These loads are to mimic the main forces acting on an offshore riser, for which an analytical methodology has been developed and applied. In particular, non-linear normal modes (NNMs) and non-linear multi-modes (NMMs) have been constructed by using the method of multiple scales. This is to effectively analyse the transversal vibration responses by monitoring the modal responses and mode interactions. The developed analytical models have been crosschecked against the results from FEM simulation. The FEM model having 26 elements and 77 degrees-of-freedom gave similar results as the low-dimensional (one degree-of-freedom) non-linear oscillator, which was developed by constructing a so-called invariant manifold. The comparisons of the dynamical responses were made in terms of time histories, phase portraits and mode shapes.

1. Introduction

Fatigue prediction and understanding of how a structure or its component may react to applied external loads are becoming increasingly important with greater demands on the design of modern engineering systems. Linearisation for modern structures, especially the light and flexible ones that must carry greater loads for longer periods of time, may not be sufficient because of the inexact results such an analysis would give. Consequently, non-linearities should be accounted for and included in the mathematical models, which leads to the use of non-linear normal modes (NNMs).

Rosenberg and Pak proposed the extension from linear to NNMs and gave proof of the existence of general non-linear modal motions in non-linear dynamical systems [1]. Shaw and Pierre [2] extended Rosenberg's definition to include systems with arbitrary damping and gyroscopic properties. Based on their definition they devised a technique for calculating non-linear modes of discrete [3] and continuous [4] systems where modal motion is limited to a surface in the system's phase space, a so-called invariant manifold. Like the name suggests, the invariance property of the NNMs is retained, which extends also to invariant manifolds of systems with internal resonances.

In flexible structures undergoing large amplitudes of oscillation, geometric and other non-linearities not only considerably affect dynamical behaviour but also couple modes in a manner that cause those, whose natural frequencies are (nearly) commensurate, to interact as coupled NNMs, which respond as a multi-modal periodic motion with constant relative phase [5]. Consequently, when motion at a single natural frequency is initiated, influences of the connected modes can be detected in the oscillation. There is a vast literature on the existence, evaluation and stability analysis of coupled and uncoupled normal modes of weakly non-linear systems exhibiting quadratic and cubic non-linearities [5–15]. Rega and his co-workers [16–18] used multi-modes to describe the dynamical behaviour of cables. Understanding the properties of systems with internal resonance helps in the prediction of coupled modes, enabling computational time to be saved, which would be especially welcome for modal analysis with finite elements. Mazzilli and co-workers implemented non-linear modes in the finite-element analysis of reticulated structures oscillating in a purely single mode [19] as well as those with internal resonances [20].

This paper aims at: (i) clarifying the formulation of the non-linear equations off motion of a continuous model of a straight beam, subjected to uniformly distributed axial load and an end axial thrust, using Hamilton's Principle; (ii) obtaining non-linear modes by means of an asymptotic analysis and (iii) comparing the analytical results with those obtained via finite-element modelling.

* Corresponding author. Tel.: +55 1130915232.
E-mail address: cenmazzi@usp.br (C.E.N. Mazzilli).

0020-7462/$ - see front matter © 2008 Elsevier Ltd. All rights reserved.
doi:10.1016/j.ijnonlinmec.2008.04.004

With respect to (i), classical simplifying assumptions, such as neglecting longitudinal inertial forces and averaging geometric stiffness effects along the beam, as already proposed by a number of authors—see Kauderer [21], Nayfeh and Nayfeh [22], Nayfeh et al. [23] and Singh et al. [24]—lead to an equation of motion for the transversal displacement, which is de-coupled from the longitudinal one.

Then, referring to (ii), the method of multiple scales is used to determine the NNMs, considering both bending and geometric stiffness effects. It is found that these modes are similar to the linear ones, as far as the transversal motion is concerned. In other words, the invariant manifold that characterises the NNM coincides with the corresponding linear-mode eigenplane, though a non-linear oscillator rules the system dynamics—see Shaw and Pierre [2,3] and Shaw et al. [25]. Further, due to the quasi-rational relationship between the linear natural frequencies, a number of internal resonances may arise, which would require consideration of non-linear multi-modes (NMMs)—see Baracho et al. [19,20]. Again, the method of multiple scales is used to investigate a particular NMM, which couples the first and the third linear modes.

The obtained analytical solutions, after the approximations incurred, obviously have shortcomings, especially for long beams, such as those of typical vertical offshore risers, which are seen when they are compared to non-linear finite-element results—see Sanches et al. [26] and Soares and Mazzilli [27]. A critical appraisal of the discrepancies found emphasises the role played by the constant normal force hypothesis in the analytical model, which is the purpose of (iii).

Although outside the paper scope, non-linear modes are expected to be a useful tool when modelling forced vibrations of slender structural systems with a huge number of degrees-of-freedom (DOF), since they may provide efficient projecting functions for number of DOF reduction—see Shaw et al. [25] and Mazzilli et al. [28]—thus allowing for a smaller computational effort. This is the case, for instance, of vertical offshore risers subjected to fluid-dynamic instabilities [29–32], such as those caused by vortex-induced vibrations (VIVs).

The paper is organised as follows. Next, the non-linear equations of an axially loaded Bernoulli–Euler beam are derived. In Sections 3 and 4, NNMs and NMMs are developed, by using a combination of a perturbation method and the invariant manifold approach. The developed methodology is applied in Section 5 to the case study of a pinned–pinned riser beam.

2. Non-linear equations of motion of an axially loaded beam

In this section the non-linear equations of motion of an axially loaded beam are presented, as they appear following a Hamiltonian procedure—see Pars [33] and Meirovitch [34]. Fig. 1(a) introduces the basic notation, whereas Fig. 1(b) refers to the kinematics of the Bernoulli–Euler beam model.

Here, m and p are the mass and the axial load per unit length, and EA and EI are the axial and flexural rigidity. The Bernoulli–Euler kinematical assumption leads to the following expressions for the displacements of a generic point P:

$$u_p = u - z\sin\varphi \cong u - zw',$$

$$w_p = w + z(\cos\varphi - 1) \cong w,$$

$$\varphi = \arctan\left(\frac{w'}{1+u'}\right) \cong w'. \tag{1}$$

Primes denote differentiation with respect to the axial co-ordinate. The Lagrangian and the engineering strains are assumed to be identical for practical purposes, provided they are small. The strain at a generic point P of the riser along the longitudinal direction is

$$\varepsilon_P = u'_P + \tfrac{1}{2}(u'_P)^2 + \tfrac{1}{2}(w'_P)^2 \cong u' - zw'' + \tfrac{1}{2}(w')^2 = \varepsilon - zw'', \tag{2}$$

where ε is the axial strain:

$$\varepsilon = u' + \tfrac{1}{2}(w')^2. \tag{3}$$

The assumption that $u_p = O(w_P^2)$ is implicit in the approximation introduced in (2). Eq. (4) of transversal motion has been derived using the Hamilton's Principle. Overdots indicate differentiation with respect to time. Details of all steps undertaken to arrive at Eq. (4) are given in Appendix A.

$$m\ddot{w} + \mathrm{EI}\,w^{\mathrm{IV}} - \mathrm{EA}\left[\frac{u_\ell - u_0}{\ell} + \frac{1}{2\ell}\int_0^\ell w'^2\,\mathrm{d}x + \frac{p}{\mathrm{EA}}\left(\frac{\ell}{2} - x\right)\right]w'' + pw' = 0. \tag{4}$$

Here, *two different problems* can be distinguished, namely that of an imposed axial displacement or an imposed thrust at the beam-ends. In the *first one*, supposing that the right end is fixed, that is, $u_\ell = 0$, a tensile axial force $N_0(0)$ is applied to the originally rectilinear beam at its left end in time $t = 0$ together with the rightward-distributed axial load p, still resulting a certain leftward axial displacement $-u_0$, before the onset of transversal vibration. The left end is then fixed, that is, $u_0(t) = -u_0 = \text{const.}$, so that once the transversal oscillation takes place, the axial force at the left end varies with time (as a matter of fact, $N_0(t) \geqslant N_0(0)$, due to the axial strain increase caused by bending):

$$N_0(t) = N_0(0) + \frac{\mathrm{EA}}{2\ell}\int_0^\ell w'^2\,\mathrm{d}x, \tag{5}$$

where

$$N_0(0) = -\frac{\mathrm{EA}\,u_0}{\ell} + \frac{p\ell}{2}. \tag{6}$$

Note that the axial force along the beam length for any time is given by

$$N(x,t) = N_0(t) - px = -\frac{\mathrm{EA}\,u_0}{\ell} + p\left(\frac{\ell}{2} - x\right) + \frac{\mathrm{EA}}{2\ell}\int_0^\ell w'^2\,\mathrm{d}x. \tag{7}$$

Taking Eq. (7) into consideration, Eq. (4) can be concisely rewritten as

$$m\ddot{w} + \mathrm{EI}\,w^{\mathrm{IV}} - N(x,t)w'' + pw' = 0. \tag{8}$$

A further approximation is now introduced to eliminate the spatial dependence of $N(x,t)$ by taking its average value along the beam in Eq. (7), when solving Eq. (8), that is

$$m\ddot{w} + \mathrm{EI}\,w^{\mathrm{IV}} - \bar{N}w'' - \frac{\mathrm{EA}}{2\ell}w''\int_0^\ell w'^2\,\mathrm{d}x + pw' = 0, \tag{9}$$

where

$$\bar{N} = N_0(0) - \frac{p\ell}{2} = -\frac{\mathrm{EA}\,u_0}{\ell}. \tag{10}$$

Once w is determined from Eq. (9), the axial displacements can be obtained from Eq. (A.13) as

$$u(x,t) = -\frac{\bar{N}(\ell - x)}{\mathrm{EA}} + \frac{px(\ell - x)}{2\mathrm{EA}} - \frac{1}{2}\int_0^x \left(\frac{\mathrm{d}w}{\mathrm{d}\xi}\right)^2 \mathrm{d}\xi + \frac{x}{2\ell}\int_0^\ell w'^2\,\mathrm{d}x. \tag{11}$$

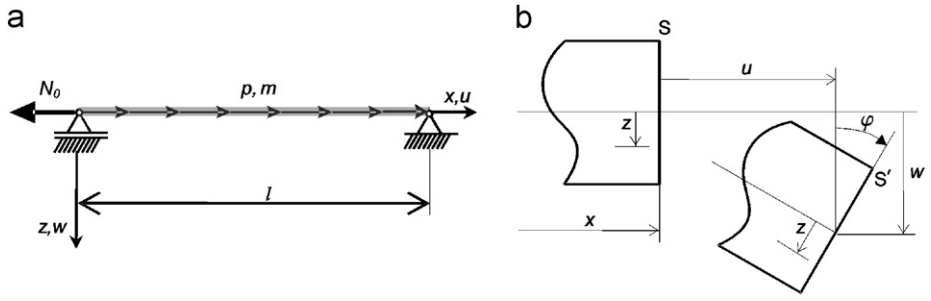

Fig. 1. (a) Schematics of an axially loaded beam with uniformly distributed load p, (b) Bernoulli–Euler beam model.

In the *second problem*, a constant axial thrust $N_0(t) = N_0 = \text{const.}$ is applied at the beam left end, while the axial displacement $u_0(t)$ is not constrained, so that Eq. (9) can be simply written as

$$m\ddot{w} + \mathrm{EI}\, w^{\mathrm{IV}} - N(x)w'' + pw' = 0, \tag{12}$$

where

$$N(x) = N_0 - px. \tag{13}$$

If the same approximation is applied, as before, to eliminate the spatial dependence of $N(x)$ in (13), the following equation of motion appears:

$$m\ddot{w} + \mathrm{EI}\, w^{\mathrm{IV}} - \bar{N}w'' + pw' = 0. \tag{14}$$

It is to be reckoned that, although Eq. (14) is a linear equation, the axial displacement will still be a non-linear function of the transversal displacement amplitudes. In particular, at the beam left end it will be

$$u_0(t) = -\frac{N_0\ell}{\mathrm{EA}} + \frac{p\ell^2}{2\mathrm{EA}} + \frac{1}{2}\int_0^\ell w'^2\, \mathrm{d}x. \tag{15}$$

As compared to the *first problem*, the *second* one has a weaker geometric stiffness. Therefore, the transversal amplitudes and velocities are expected to be larger in the *second problem* than those in the *first problem*. In this paper, only the *first problem* will be dealt with in the analytical analysis using the method of multiple scales—see Nayfeh [22,35]. It is to be reckoned that the strong simplifying assumption of constant normal force will probably be the main reason for the differences found between the results of the analytical and the finite-element models (FEMs) considered in Section 5.

Therefore, Eq. (9) is conveniently rewritten as

$$\ddot{w} + \alpha w^{\mathrm{IV}} - \beta w'' - \mu w'' \int_0^\ell w'^2\, \mathrm{d}x + \varepsilon^3\gamma w' = 0, \tag{16}$$

where

$$\alpha = \frac{\mathrm{EI}}{m}, \quad \beta = \frac{\bar{N}}{m}, \quad \mu = \frac{\mathrm{EA}}{2m\ell}, \quad \varepsilon^3\gamma = \frac{p}{m}, \quad 0 < \varepsilon < 1.$$

The term p/m in Eq. (16) has been conveniently scaled as one of order $O(\varepsilon^3)$, where ε from now on will stand for the book-keeping parameter of the perturbation analysis, because it is much smaller than α and β for usual design parameters—see Section 5.

According to the method of multiple scales, the solution will be sought in the form

$$w(x,t) = \varepsilon w_1(x, T_0, T_1 \ldots) + \varepsilon^2 w_2(x, T_0, T_1 \ldots) + \cdots, \tag{17}$$

where the time scales are

$$T_j = \varepsilon^j t. \tag{18}$$

The following differential operators and relationships are introduced:

$$D_j^q = \frac{\partial^q}{\partial T_j^q},$$

$$\frac{\mathrm{d}}{\mathrm{d}t} = D_0 + \varepsilon D_1 + \varepsilon^2 D_2 + \cdots,$$

$$\frac{\mathrm{d}^2}{\mathrm{d}t^2} = D_0^2 + \varepsilon 2D_0D_1 + \varepsilon^2(D_1^2 + 2D_0D_2) + \cdots. \tag{19}$$

Substituting Eqs. (17)–(19) into Eq. (16) and collecting terms of the same order of ε, it is possible to arrive at differential equations whose solutions and solvability conditions allow for the characterisation of the NNMs.

Order ε solution

The equation of order ε leads to

$$D_0^2 w_1 + \alpha w_1^{\mathrm{IV}} - \beta w_1'' = 0 \tag{20}$$

with the boundary conditions $w_1(0) = w_1(\ell) = w_1''(0) = w_1''(\ell) = 0$. So, the solution w_1 can be written in the form

$$w_1(x, T_0, T_1 \ldots) = \sum_k w_{1k}(x, T_0, T_1 \ldots),$$

$$w_{1k}(x, T_0, T_1 \ldots) = A_{1k}(T_0, T_1 \ldots) \sin\frac{k\pi x}{\ell}. \tag{21}$$

After substituting Eq. (21) into Eq. (20), it is obtained

$$D_0^2 A_{1k} + \omega_k^2 A_{1k} = 0, \quad \omega_k = \frac{k\pi}{\ell}\sqrt{\beta + \frac{\alpha k^2\pi^2}{\ell^2}}, \tag{22}$$

where ω_k is the frequency of the linear mode k, taking into account both the riser geometric and bending stiffness. It should be noticed that the geometric stiffness effect is larger at the left end, where the normal force is larger, and decreases rightwards. In Eq. (22) an average geometric stiffness was used, as it is clear from the definition for β in Eq. (16). The solution for Eq. (22) can be written in complex variables as

$$A_{1k} = Y_k(T_1, T_2 \ldots)\mathrm{e}^{\mathrm{i}\omega_k T_0} + \mathrm{cc}. \tag{23}$$

For long beams, such as offshore risers, the geometric stiffness β largely prevails over the bending stiffness α, so that there is an almost linear relationship between ω_k and the mode number k. Therefore, due to the almost commensurability of the natural frequencies, the linear modes can be strongly coupled, thus favouring internal resonance. Besides other possibilities of internal resonance, it is of particular interest that one of the 1:3 type between modes $1, 3, 9, 27\ldots$ or $2, 6, 18\ldots$.

3. Non-linear normal modes

A NNM is a non-linear system free-vibration motion about its static equilibrium configuration, which takes place on a two-dimensional invariant manifold embedded in the phase space, so that it is tangent at the equilibrium point to the corresponding linear system eigenplane—see Shaw and Pierre [2,3]. Hence, once the initial conditions have set a motion on this manifold, it will stay there. The NNM will be evaluated as the solution Eq. (17) is found following the next steps of the method of multiple scales. After collecting terms of order ε^2 in Eq. (16), one gets:

Order ε^2 solution

$$D_0^2 w_{2k} + \alpha w_{2k}^{\mathrm{IV}} - \beta w_{2k}'' = -2D_0 D_1 w_{1k}. \tag{24}$$

The solvability condition requires that $D_1 Y_k = 0$, hence $Y_k = Y_k(T_2, \ldots)$. Also, the homogeneous solution w_{2k} is already included in w_{1k}. After collecting terms of order ε^3 in Eq. (16), one gets:

Order ε^3 solution

$$\begin{aligned} &D_0^2 w_{3k} + \alpha w_{3k}^{\mathrm{IV}} - \beta w_{3k}'' \\ &= -2D_0 D_2 w_{1k} + \mu w_{1k}'' \int_0^{\ell} w_{1k}'^2 \,\mathrm{d}x \\ &= [-2\mathrm{i}\omega_k \mathrm{e}^{\mathrm{i}\omega_k T_0} D_2 Y_k - \Lambda_k (Y_k^3 \mathrm{e}^{\mathrm{i}3\omega_k T_0} \\ &\quad + 3Y_k^2 \bar{Y}_k \mathrm{e}^{\mathrm{i}\omega_k T_0})] \sin \frac{k\pi x}{\ell}, \end{aligned} \tag{25}$$

where

$$\Lambda_k = \left(\frac{\mu\ell}{2}\right) \frac{k^4\pi^4}{\ell^4} = \left(\frac{\mathrm{EA}}{4m}\right) \frac{k^4\pi^4}{\ell^4}. \tag{26}$$

Eq. (25) requires the following solvability condition:

$$-2\mathrm{i}\omega_k D_2 Y_k - 3\Lambda_k Y_k^2 \bar{Y}_k = 0. \tag{27}$$

In order to determine a solution for Eq. (27), let Y_k be written in the form

$$Y_k = \tfrac{1}{2} a_k \mathrm{e}^{\mathrm{i}\theta_k}, \quad a_k, \theta_k \in \Re. \tag{28}$$

One finds out that

$$a_k = a_k(T_3), \quad \theta_k = \theta_{0k}(T_3) + \frac{3\Lambda_k}{8\omega_k} a_k^2 T_2. \tag{29}$$

By considering the solutions w_{1k}, w_{2k} and w_{3k}, the k-th NNM is thus defined in the time domain as

$$\begin{aligned} w_k(x,t) &= (\varepsilon a_k) \left\{ \cos(\Omega_k t + \theta_{0k}) \right. \\ &\quad \left. + \frac{\Lambda_k (\varepsilon a_k)^2}{32\omega_k^2} \cos 3(\Omega_k t + \theta_{0k}) \right\} \sin \frac{k\pi x}{\ell} + O(\varepsilon^4), \\ u_k(x,t) &= -\frac{k\pi}{8\ell} (\varepsilon a_k)^2 \left\{ \cos(\Omega_k t + \theta_{0k}) \right. \\ &\quad \left. + \frac{\Lambda_k (\varepsilon a_k)^2}{32\omega_k^2} \cos 3(\Omega_k t + \theta_{0k}) \right\}^2 \sin \frac{2k\pi x}{\ell} \\ &\cong -\frac{k\pi}{16\ell} (\varepsilon a_k)^2 [1 + \cos 2(\Omega_k t + \theta_{0k})] \sin \frac{2k\pi x}{\ell} \\ &\quad + O(\varepsilon^4), \end{aligned} \tag{30}$$

where εa_k is the amplitude of the associated k-th linear mode and

$$\Omega_k = \omega_k \left[1 + \frac{3\Lambda_k}{8\omega_k^2} (\varepsilon a_k)^2 \right]. \tag{31}$$

Eq. (31) establishes the frequency–amplitude relationship for the k-th non-linear mode. In the above solution, the influence of the distributed axial load is restricted to the value of the average normal force along the beam $\bar{N}$, as defined in Eq. (10). Further influence would appear with terms of order $O(\varepsilon^4)$, by means of $(p/m)w'$. As anticipated, the geometric stiffness of the so-called *first problem* is larger than that of the *second problem* and of the *linearised problem*, as well, and this is confirmed by the increase in the frequency Ω_k, due to increasing vibration amplitudes, as observed in Eq. (31).

Construction of invariant manifold: The NNMs can be characterised by writing the displacements and velocities as functions of two *ad hoc* chosen modal variables. For this purpose, consider the following modal variables:

$$U_k(t) = w_k(\bar{x}, t), \quad V_k(t) = \dot{U}_k(t), \tag{32}$$

so that $\bar{x}$ is such that

$$\sin\left(\frac{k\pi}{\ell}\right) \bar{x} = 1. \tag{33}$$

In this way, displacements for the k-th NNM can be written in terms of the modal variables as follows:

$$w_k(x,t) = F_{1k}^w(x) U_k(t), \quad u_k(x,t) = F_{3k}^u(x) U_k^2(t). \tag{34}$$

Note that this corresponds to a similar mode, at least as far as the transversal displacement is considered alone! Recasting now Eq. (34), the velocities for the NNM can be written in terms of the modal variables as follows:

$$\dot{w}_k = G_{2k}^w V_k, \quad \dot{u}_k = G_{4k}^u U_k V_k, \tag{35}$$

where

$$F_{1k}^w(x) = G_{2k}^w = \sin \frac{k\pi x}{\ell}, \tag{36}$$

$$F_{3k}^u(x) = \frac{1}{2} G_{4k}^u = -\frac{k\pi}{8\ell} \sin \frac{2k\pi x}{\ell}. \tag{37}$$

Within the invariant manifold, the equation of the modal oscillator is

$$\ddot{U}_k + \omega_k^2 U_k + \varepsilon^2 \Lambda_k U_k^3 = 0, \tag{38}$$

where, as already seen, $\omega_k = (k\pi/\ell)\sqrt{\beta + \alpha k^2\pi^2/\ell^2}$ and $\Lambda_k = (\mu\ell/2)k^4\pi^4/\ell^4 = (\mathrm{EA}/4m)k^4\pi^4/\ell^4$.

Notice that

$$w(x,t) = \sum_k w_k(x,t), \quad u(x,t) = u_e + \sum_k u_k(x,t), \tag{39}$$

where

$$u_e = -\frac{N_0(\ell - x)}{\mathrm{EA}} + \frac{px}{2\mathrm{EA}}(\ell - x). \tag{40}$$

4. Non-linear multi-modes

A NMM, coupling n normal modes, is a non-linear system free-vibration motion about a static equilibrium configuration, which takes place on a $2n$-dimensional invariant manifold embedded in the phase space, so that it is tangent at the equilibrium point to the n corresponding linear system eigenplanes—see Shaw et al. [25] and Nayfeh [36]. Hence, once the initial conditions have set a motion on this manifold, it will stay there. The NMM will be evaluated as the

solution Eq. (17) is found following the steps of the method of multiple scales.

Order ε solution

If only terms of order ε are retained in Eq. (16), the following free-vibration problem appears:

$$D_0^2 w_1 + \alpha w_1^{\mathrm{IV}} - \beta w_1'' = 0. \tag{41}$$

As seen before, the solution of the above equation for the k-th mode reads

$$w_{1k} = Y_k(T_2)\mathrm{e}^{\mathrm{i}\omega_k T_0} \sin\frac{k\pi x}{\ell} + \mathrm{cc}. \tag{42}$$

Now, a multi-mode that only couples the first and the third modes is considered. The two resonating modes of smaller and larger frequency will be assigned indices I and II. To the order of ε, the time response of a free-vibration motion, which solely contains contributions from these two modes, can be written as

$$w_1 = Y_{\mathrm{I}}(T_2)\mathrm{e}^{\mathrm{i}\omega_{\mathrm{I}} T_0} \sin\frac{\pi x}{\ell} + Y_{\mathrm{II}}(T_2)\mathrm{e}^{\mathrm{i}\omega_{\mathrm{II}} T_0} \sin\frac{3\pi x}{\ell} + \mathrm{cc}, \tag{43}$$

where

$$\omega_{\mathrm{II}} = 3\omega_{\mathrm{I}}. \tag{44}$$

By imposing the solution to be of the form Eq. (43), it is being assumed that the phase trajectory stays on the invariant manifold that is tangent to the eigenplane defined by the first and the third linear modes in the phase plane.

Order ε^2 solution

Following the same approach presented in Section 3, the following result comes out from the corresponding solvability conditions:

$$Y_{\mathrm{I}} = Y_{\mathrm{I}}(T_2), \quad Y_{\mathrm{II}} = Y_{\mathrm{II}}(T_2). \tag{45}$$

Order ε^3 solution

After collecting terms of order ε^3, it can be seen that

$$D_0^2 w_3 + \alpha w_3^{\mathrm{IV}} - \beta w_3'' = -2D_0 D_2 w_1 + \mu w_1'' \int_0^{\ell} (w_1')^2 \,\mathrm{d}x. \tag{46}$$

Solution of Eq. (46) is sought in the form

$$w_3 = A_{3,\mathrm{I}} \sin\frac{\pi x}{\ell} + A_{3,\mathrm{II}} \sin\frac{3\pi x}{\ell}. \tag{47}$$

Substituting Eq. (47) into Eq. (46) gives

$$\begin{aligned}
&(D_0^2 A_{3,\mathrm{I}} + \omega_{\mathrm{I}}^2 A_{3,\mathrm{I}}) \sin\frac{\pi x}{\ell} + (D_0^2 A_{3,\mathrm{II}} + \omega_{\mathrm{II}}^2 A_{3,\mathrm{II}}) \sin\frac{3\pi x}{\ell} \\
&\quad = -2\mathrm{i}\omega_{\mathrm{I}}(D_2 Y_{\mathrm{I}}\mathrm{e}^{\mathrm{i}\omega_{\mathrm{I}} T_0} + \mathrm{cc}) \sin\frac{\pi x}{\ell} \\
&\qquad - 2\mathrm{i}\omega_{\mathrm{II}}(D_2 Y_{\mathrm{II}}\mathrm{e}^{\mathrm{i}\omega_{\mathrm{II}} T_0} + \mathrm{cc}) \sin\frac{3\pi x}{\ell} \\
&\qquad - \frac{\pi^4 \mu}{2\ell^3}(Y_{\mathrm{I}}\mathrm{e}^{\mathrm{i}\omega_{\mathrm{I}} T_0} + \mathrm{cc})(Y_{\mathrm{I}}^2\mathrm{e}^{2\mathrm{i}\omega_{\mathrm{I}} T_0} \\
&\qquad + Y_{\mathrm{I}}\bar{Y}_{\mathrm{I}} + 9Y_{\mathrm{II}}^2\mathrm{e}^{2\mathrm{i}\omega_{\mathrm{II}} T_0} + 9Y_{\mathrm{II}}\bar{Y}_{\mathrm{II}} + \mathrm{cc}) \sin\frac{\pi x}{\ell} \\
&\qquad - \frac{9\pi^4 \mu}{2\ell^3}(Y_{\mathrm{II}}\mathrm{e}^{\mathrm{i}\omega_{\mathrm{II}} T_0} + \mathrm{cc})(Y_{\mathrm{I}}^2\mathrm{e}^{2\mathrm{i}\omega_{\mathrm{I}} T_0} + Y_{\mathrm{I}}\bar{Y}_{\mathrm{I}} + 9Y_{\mathrm{II}}^2\mathrm{e}^{2\mathrm{i}\omega_{\mathrm{II}} T_0} \\
&\qquad + 9Y_{\mathrm{II}}\bar{Y}_{\mathrm{II}} + \mathrm{cc}) \sin\frac{3\pi x}{\ell}.
\end{aligned} \tag{48}$$

Firstly, the terms with $\sin \pi x/\ell$ on both sides of Eq. (48) are equated, which yields

$$\begin{aligned}
&D_0^2 A_{3,\mathrm{I}} + \omega_{\mathrm{I}}^2 A_{3,\mathrm{I}} \\
&\quad = -2\mathrm{i}\omega_{\mathrm{I}}(D_2 Y_{\mathrm{I}}\mathrm{e}^{\mathrm{i}\omega_{\mathrm{I}} T_0} + \mathrm{cc}) \\
&\qquad - \frac{\pi^4 \mu}{2\ell^3}(Y_{\mathrm{I}}\mathrm{e}^{\mathrm{i}\omega_{\mathrm{I}} T_0} + \mathrm{cc})(Y_{\mathrm{I}}^2\mathrm{e}^{2\mathrm{i}\omega_{\mathrm{I}} T_0} + Y_{\mathrm{I}}\bar{Y}_{\mathrm{I}} \\
&\qquad + 9Y_{\mathrm{II}}^2\mathrm{e}^{2\mathrm{i}\omega_{\mathrm{II}} T_0} + 9Y_{\mathrm{II}}\bar{Y}_{\mathrm{II}} + \mathrm{cc}).
\end{aligned} \tag{49}$$

Then the terms with $\sin 3\pi x/\ell$ on both sides of Eq. (48) are equated giving

$$\begin{aligned}
&D_0^2 A_{3,\mathrm{II}} + \omega_{\mathrm{II}}^2 A_{3,\mathrm{II}} \\
&\quad = -2\mathrm{i}\omega_{\mathrm{II}}(D_2 Y_{\mathrm{II}}\mathrm{e}^{\mathrm{i}\omega_{\mathrm{II}} T_0} + \mathrm{cc}) \\
&\qquad - \frac{9\pi^4 \mu}{2\ell^3}(Y_{\mathrm{II}}\mathrm{e}^{\mathrm{i}\omega_{\mathrm{II}} T_0} + \mathrm{cc})(Y_{\mathrm{I}}^2\mathrm{e}^{2\mathrm{i}\omega_{\mathrm{I}} T_0} + Y_{\mathrm{I}}\bar{Y}_{\mathrm{I}} \\
&\qquad + 9Y_{\mathrm{II}}^2\mathrm{e}^{2\mathrm{i}\omega_{\mathrm{II}} T_0} + 9Y_{\mathrm{II}}\bar{Y}_{\mathrm{II}} + \mathrm{cc}).
\end{aligned} \tag{50}$$

Now, the elimination of secular terms in Eqs. (49) and (50) should be enforced, leading to

$$\begin{aligned}
&-2\mathrm{i}\omega_{\mathrm{I}} D_2 Y_{\mathrm{I}} - 3\Lambda_1 Y_{\mathrm{I}}^2 \bar{Y}_{\mathrm{I}} - 18\Lambda_1 Y_{\mathrm{I}} Y_{\mathrm{II}} \bar{Y}_{\mathrm{II}} = 0, \\
&-2\mathrm{i}\omega_{\mathrm{II}} D_2 Y_{\mathrm{II}} - 18\Lambda_1 Y_{\mathrm{I}} \bar{Y}_{\mathrm{I}} Y_{\mathrm{II}} - 243\Lambda_1 Y_{\mathrm{II}}^2 \bar{Y}_{\mathrm{II}} = 0,
\end{aligned} \tag{51}$$

where Λ_1 comes from Eq. (26), with $k=1$. The solution is sought as in Eq. (28). After real and imaginary parts are separated, the following set of first-order differential equations is integrated:

$$\begin{aligned}
&D_2 a_{\mathrm{I}} = 0 \Rightarrow a_{\mathrm{I}} = \mathrm{const}, \quad D_2 a_{\mathrm{II}} = 0 \Rightarrow a_{\mathrm{II}} = \mathrm{const}, \\
&\omega_{\mathrm{I}} a_{\mathrm{I}} D_2\theta_{\mathrm{I}} - \frac{3\Lambda_1}{8} a_{\mathrm{I}}^3 - \frac{18\Lambda_1}{8} a_{\mathrm{I}} a_{\mathrm{II}}^2 = 0 \\
&\quad \Rightarrow \theta_{\mathrm{I}} = \theta_{\mathrm{I},0} + \frac{\Lambda_1}{8\omega_{\mathrm{I}}}(3a_{\mathrm{I}}^2 + 18a_{\mathrm{II}}^2)T_2, \\
&\omega_{\mathrm{II}} a_{\mathrm{II}} D_2\theta_{\mathrm{II}} - \frac{18\Lambda_1}{8} a_{\mathrm{I}}^2 a_{\mathrm{II}} - \frac{243\Lambda_1}{8} a_{\mathrm{II}}^3 = 0 \\
&\quad \Rightarrow \theta_{\mathrm{II}} = \theta_{\mathrm{II},0} + \frac{\Lambda_1}{8\omega_{\mathrm{II}}}(18a_{\mathrm{I}}^2 + 243a_{\mathrm{II}}^2)T_2.
\end{aligned} \tag{52}$$

Hence

$$\begin{aligned}
A_{3,\mathrm{I}} &= \frac{\Lambda_1}{8\omega_{\mathrm{I}}^2} Y_{\mathrm{I}}^3 \mathrm{e}^{3\mathrm{i}\omega_{\mathrm{I}} T_0} + \frac{9\Lambda_1}{24\omega_{\mathrm{I}}^2} \bar{Y}_{\mathrm{I}} Y_{\mathrm{II}}^2 \mathrm{e}^{\mathrm{i}(2\omega_{\mathrm{II}} - \omega_{\mathrm{I}})T_0} \\
&\quad + \frac{9\Lambda_1}{48\omega_{\mathrm{I}}^2} Y_{\mathrm{I}} Y_{\mathrm{II}}^2 \mathrm{e}^{\mathrm{i}(2\omega_{\mathrm{II}} + \omega_{\mathrm{I}})T_0} + \mathrm{cc}, \\
A_{3,\mathrm{II}} &= -\frac{9\Lambda_1}{8\omega_{\mathrm{I}}^2} \bar{Y}_{\mathrm{I}}^2 Y_{\mathrm{II}} \mathrm{e}^{\mathrm{i}(\omega_{\mathrm{II}} - 2\omega_{\mathrm{I}})T_0} + \frac{9\Lambda_1}{16\omega_{\mathrm{I}}^2} Y_{\mathrm{I}}^2 Y_{\mathrm{II}} \mathrm{e}^{\mathrm{i}(\omega_{\mathrm{II}} + 2\omega_{\mathrm{I}})T_0} \\
&\quad + \frac{81\Lambda_1}{72\omega_{\mathrm{I}}^2} Y_{\mathrm{II}}^3 \mathrm{e}^{3\mathrm{i}\omega_{\mathrm{II}} T_0} + \mathrm{cc}.
\end{aligned} \tag{53}$$

The NMM that couples the first and the third linear modes is described by Eqs. (54) and (55). Obviously, Eq. (31) is a particular case of Eq. (55) and both equations indicate that the non-linear system has larger modal frequencies and smaller periods, as compared to the linearised one, i.e. it stiffens with increasing amplitudes. Small corrections to the vibration amplitudes of the linear solution

also apply.

$$
\begin{aligned}
&w_{\mathrm{I,II}}(x,t)\\
&\quad=(\varepsilon a_{\mathrm{I}})\left[\cos(\Omega_{\mathrm{I}}t+\theta_{\mathrm{I},0})+\frac{\Lambda_1}{32\omega_{\mathrm{I}}^2}(\varepsilon a_{\mathrm{I}})^2\cos 3(\Omega_{\mathrm{I}}t+\theta_{\mathrm{I},0})\right]\\
&\qquad\times\sin\frac{\pi x}{\ell}+(\varepsilon a_{\mathrm{I}})(\varepsilon a_{\mathrm{II}})^2\left\{\frac{9\Lambda_1}{96\omega_{\mathrm{I}}^2}\cos[(2\Omega_{\mathrm{II}}-\Omega_{\mathrm{I}})t\right.\\
&\qquad+2\theta_{\mathrm{II},0}-\theta_{\mathrm{I},0}]+\frac{9\Lambda_1}{192\omega_{\mathrm{I}}^2}\cos[(2\Omega_{\mathrm{II}}+\Omega_{\mathrm{I}})t\\
&\qquad\left.+2\theta_{\mathrm{II},0}+\theta_{\mathrm{I},0}]\right\}\sin\frac{\pi x}{\ell}+(\varepsilon a_{\mathrm{II}})\left[\cos(\Omega_{\mathrm{II}}t+\theta_{\mathrm{II},0})\right.\\
&\qquad\left.+\frac{81\Lambda_1}{288\omega_{\mathrm{I}}^2}(\varepsilon a_{\mathrm{II}})^2\cos 3(\Omega_{\mathrm{II}}t+\theta_{\mathrm{II},0})\right]\sin\frac{3\pi x}{\ell}\\
&\qquad+(\varepsilon a_{\mathrm{II}})(\varepsilon a_{\mathrm{I}})^2\left\{\frac{9\Lambda_1}{64\omega_{\mathrm{I}}^2}\cos[(\Omega_{\mathrm{II}}+2\Omega_{\mathrm{I}})t+\theta_{\mathrm{II},0}+2\theta_{\mathrm{I},0}]\right.\\
&\qquad\left.-\frac{9\Lambda_1}{32\omega_{\mathrm{I}}^2}\cos[(\Omega_{\mathrm{II}}-2\Omega_{\mathrm{I}})t+\theta_{\mathrm{II},0}-2\theta_{\mathrm{I},0}]\right\}\sin\frac{3\pi x}{\ell},
\end{aligned}
\tag{54}
$$

$$
\begin{aligned}
&u_{\mathrm{I,II}}(x,t)\\
&\quad=-\frac{\pi}{16\ell}(\varepsilon a_{\mathrm{I}})^2[1+\cos 2(\Omega_{\mathrm{I}}t+\theta_{\mathrm{I},0})]\sin\frac{2\pi x}{\ell}\\
&\qquad-\frac{3\pi}{16\ell}(\varepsilon a_{\mathrm{II}})^2[1+\cos 2(\Omega_{\mathrm{II}}t+\theta_{\mathrm{II},0})]\sin\frac{6\pi x}{\ell}\\
&\qquad-\frac{3\pi}{8\ell}(\varepsilon a_{\mathrm{I}})(\varepsilon a_{\mathrm{II}})\cos(\Omega_{\mathrm{I}}t+\theta_{\mathrm{I},0})\cos(\Omega_{\mathrm{II}}t+\theta_{\mathrm{II},0})\\
&\qquad\times\left(2\sin\frac{2\pi x}{\ell}+\sin\frac{4\pi x}{\ell}\right)+O(\varepsilon^4),
\end{aligned}
$$

$$
\begin{aligned}
\Omega_{\mathrm{I}}&=\omega_{\mathrm{I}}+\frac{\Lambda_1}{8\omega_{\mathrm{I}}}[3(\varepsilon a_{\mathrm{I}})^2+18(\varepsilon a_{\mathrm{II}})^2],\\
\Omega_{\mathrm{II}}&=\omega_{\mathrm{II}}+\frac{\Lambda_1}{8\omega_{\mathrm{II}}}[18(\varepsilon a_{\mathrm{I}})^2+243(\varepsilon a_{\mathrm{II}})^2].
\end{aligned}
\tag{55}
$$

5. Case study

The outcomes of Sections 3 and 4 are here applied to the analysis of a vertical riser subjected to pre-stressing and immersed weight. It is reckoned that further investigations should still be carried out to take into account the hydrodynamic effects with surrounding and inside flowing fluid, which makes the assumption of negligible inertial forces in the axial direction questionable. In the case of an immersed riser, m should account for water or oil inside it, plus the added mass of surrounding water. Table 1 lists the chosen system parameters.

Fig. 2 represents a FEM of the riser, detailing the DOF and the boundary conditions. A model having 26 elements and 77 DOFs was chosen for numerical simulation. It requires about 17 h of processing time in a PC with 2 GB RAM memory and 1.6 GHz processor for a typical non-linear mode analysis.

From the analytical result Eq. (38), it is clear that the equation of motion of the first non-linear modal oscillator is:

$$\ddot{U}+2.90\times10^{-2}U+3.81\times10^{-5}U^3=0, \tag{56}$$

where $U=w(0.5\ell)$ is the mid-span transversal displacement. From the finite-element procedure described in [27], it is also possible to obtain the equation of motion of the non-linear modal oscillator for $k=1$, which is

$$
\begin{aligned}
&\ddot{U}+2.70\times10^{-2}U-1.85\times10^{-14}V+7.014\times10^{-15}U^2\\
&\quad+1.09\times10^{-15}UV-2.73\times10^{-13}V^2+2.52\times10^{-4}U^3\\
&\quad-8.19\times10^{-14}U^2V-2.27\times10^{-2}UV^2\\
&\quad+1.014\times10^{-12}V^3=0,
\end{aligned}
\tag{57}
$$

Table 1
Data for a typical vertical steel riser

Young's modulus	$E=2.1\times10^{11}\,\mathrm{N/m^2}$
Riser length	$\ell=1800\,\mathrm{m}$
Cross-section area	$A=1.1021\times10^{-2}\,\mathrm{m^2}$
Cross-section moment of inertia	$I=4.72143\times10^{-5}\,\mathrm{m^4}$
Initial tension (at the top)	$N_0=2\times10^6\,\mathrm{N}$
Initial tension (at the bottom)	$N_\ell=6.914\times10^5\,\mathrm{N}$
Riser mass per unit length (water inside + added mass)	$m=141.24\,\mathrm{kg/m}$
Riser immersed weight per unit length	$p=727\,\mathrm{N/m}$

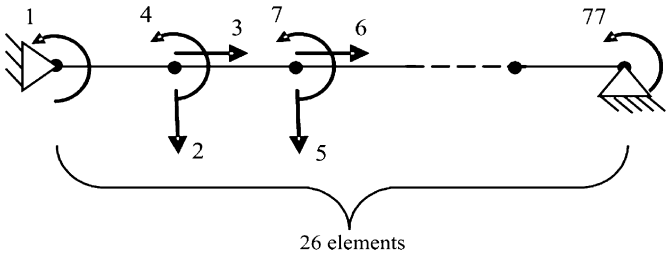

Fig. 2. Schematics of the FEM showing the number of elements and DOFs. Each node (a black dot) apart from the boundary ones was allocated three DOFs.

where $U=w(0.5\ell)$ and $V=\dot{w}(0.5\ell)$. It is readily observed from the inspection of Eq. (56), for the analytical model, and Eq. (57), for the FEM, that there are noticeable quantitative differences between both models. In fact, the coefficient of the term in U is 7% smaller in the analytical model, which leads to a 3.5% deviation in the linear frequency values. For a perfect matching of the linear frequencies, a constant normal force $N_{\mathrm{const}}=1.25\times10^6N$ should be used in the analytical solution instead of the actual average normal force $\bar{N}=1.345\times10^6N$. Further, the oscillator equation coefficient that characterises the non-linear bending stiffening effect (term in U^3) is 6.6 times larger in the FEM. Even more important, there are noticeable qualitative differences, such as the non-linear velocity-dependent term UV^2 in Eq. (57), which was not detected in the analytical solution. It is believed that all these discrepancies might be associated with the approximation, in the analytical model, of a constant normal force $\bar{N}$ along the riser length prior to the onset of transversal oscillation, in particular the loss of velocity-dependent non-linearities in the analytical model. In fact, since the geometric stiffening effect decreases and the period to complete a vibration cycle increases from top to bottom, one can guess that the NNMs nodal points are not fixed and, therefore, travelling waves along the beam should be expected, thus emphasising the influence of velocity-dependent terms. It is also interesting to observe that the velocity-dependent terms might be further connected to the term pw'/m, as seen from Eq. (16), which introduces an influence upon $w_k(x,t)$ that is in quadrature with the other terms. The numerical solution, although still considering a constant normal force within each finite element, does account for the tension variation along the riser length. Silveira et al. [37] refer to riser tension variation effects.

Fig. 3, which refers to the mid-span displacement for the first NNM, shows that the non-linear analytical solution looks still very much alike the linear one, although with an amplitude varying frequency, whereas the non-linear FEM solution displays a very distinct pattern and a ``squeezed'' phase trajectory. The increase of the initial displacement leads to lower velocities close to the static equilibrium configuration, for the FEM solution.

Fig. 4 shows a trajectory projection with respect to the displacements $p_8=w(0.12\ell)$ and $p_{32}=w(0.42\ell)$, considering the first NNM,

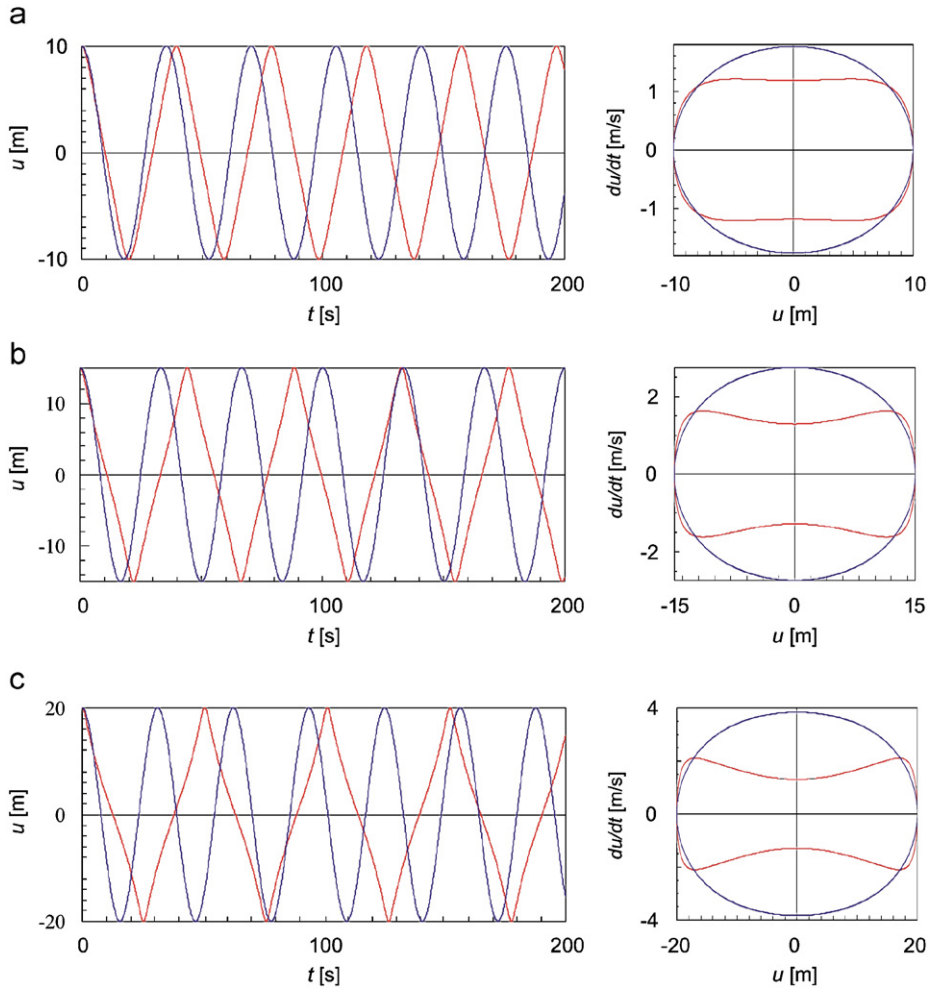

Fig. 3. Transversal mid-span displacement time responses and phase portraits (FEM: red—analytical: blue).

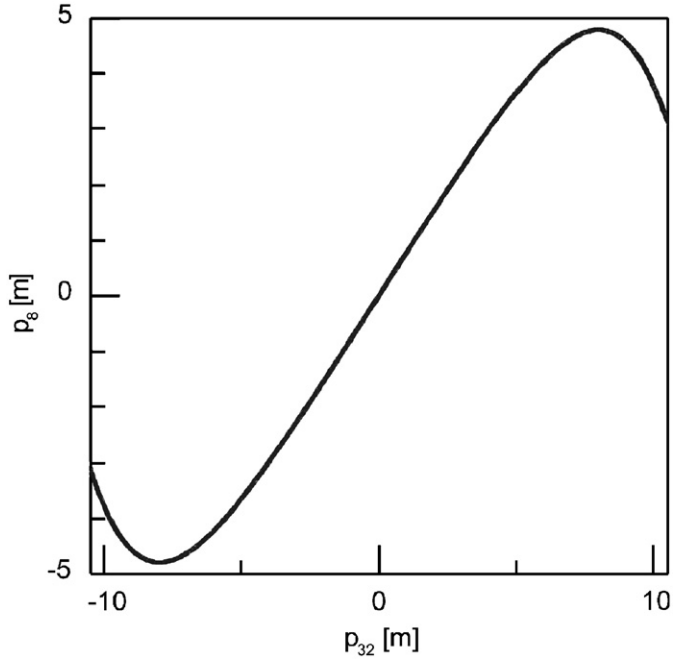

Fig. 4. Trajectory projection $p_{32} = w(0.42\ell) \times p_8 = w(0.12\ell)$ for the first non-linear normal mode.

as obtained from the FEM. From the linear theory one should expect a linear relationship between p_{32} and p_8, that is, the phase trajectory projection onto the plane $p_{32} \times p_8$ should be a straight line.

As for the multi-mode results—see Figs. 5 and 6—the analytical solution qualitatively correlates with that of the FEM reasonably well. Fig. 5 shows the trajectory projection onto the plane $p_{32} \times p_8$ and correlates coordinates that are less (p_{32}) or more (p_8) affected by the third mode. For the linear first mode, the largest displacements are expected at mid-span (near to where p_{32} is measured). As for the linear third mode, the maximum displacements would take place at $x = \ell/6$ (near to where p_8 is measured).

In Fig. 6, one finds four phase portraits $p_8 \times \dot{p}_8$ and $p_{32} \times \dot{p}_{32}$ (analytical and FEM). It is seen a smaller motion close to the initial displacement, followed by a larger motion that leads the system to a new smaller motion around a new attractor placed symmetrically to the previous one. The interaction between the two-coupled normal modes (first and third) is embodied in a sole multi-mode. Multi-modes are expected to capture the main global behaviour requiring a smaller number of DOF, for which reason they may be useful as inputs for a model-reduction technique.

Fig. 7 displays ``snapshots'' of the first and third NNMs, as well as the 1–3 multi-mode, every $\Delta t \cong T_1/12$, where T_1 is the first-mode period, as obtained from the FEM. The relative influence of each of the NNMs on the multi-mode is readily seen, as the oscillation takes place.

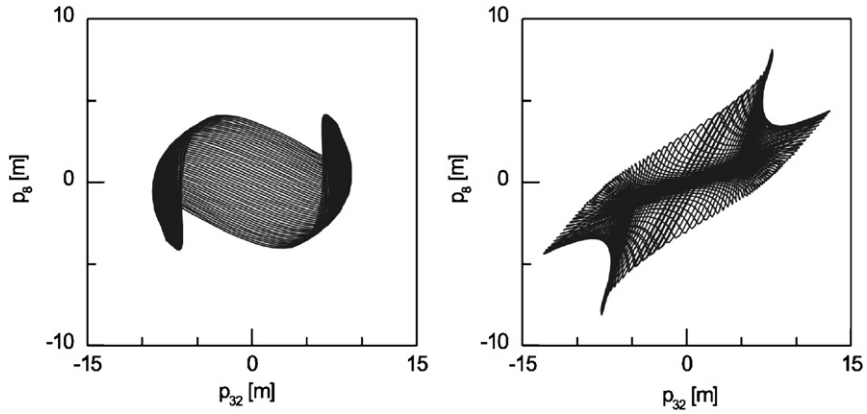

Fig. 5. Trajectory projections $p_{32} = w(0.42\ell) \times p_8 = w(0.12\ell)$ for the non-linear multi-modal interactions obtained analytically (left) and through FEM (right).

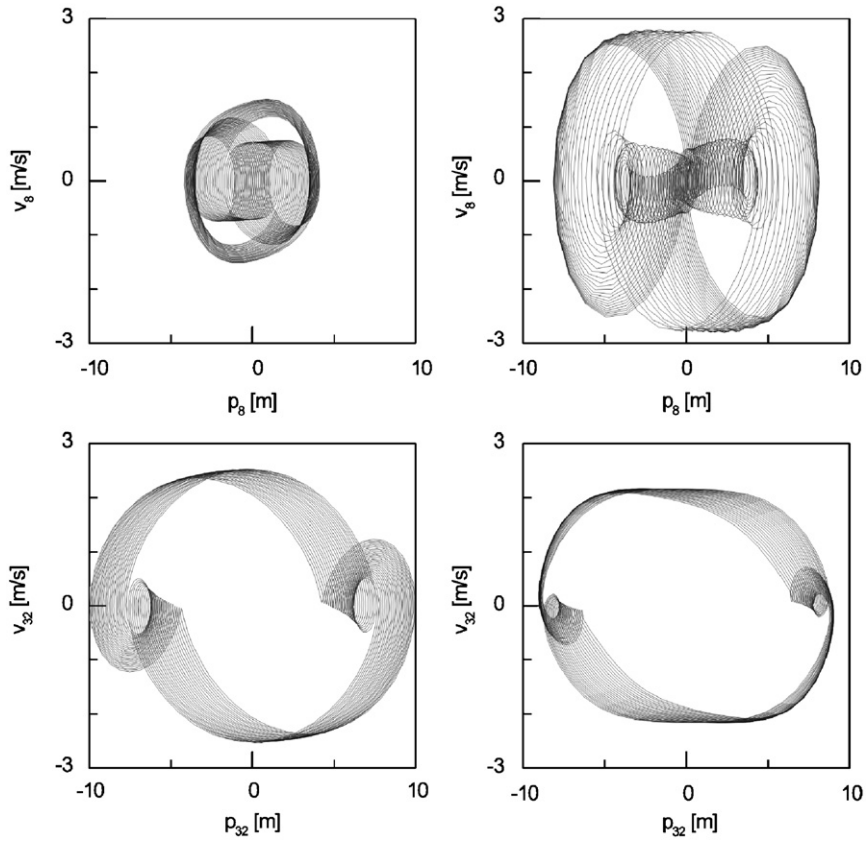

Fig. 6. Phase trajectories $p_8 \times \dot{p}_8 = v_8$ and $p_{32} \times \dot{p}_{32} = v_{32}$ for the non-linear multi-modal interactions obtained analytically (left) and through FEM (right).

6. Closing remarks

The current paper aims to rigorously derive the non-linear equations governing the dynamics of an axially loaded beam in order to develop robust low-dimensional dynamical models, which can be easily analysed. In particular, interest is placed in the complex modal interactions and how they can be effectively modified by the system parameters. The analysis is to support design and control of real structures; the application in mind is a vertical offshore riser. Derivations have helped also to clarify the formulation of the non-linear equations of motion of a continuous model of a straight beam subjected to uniformly distributed axial load and an end axial thrust, see Eq. (4) and Appendix A. The governing equations were formulated for two different loading scenarios, namely that of imposed end axial displacements or imposed end thrusts, however, only the former one was further studied by the analytical methods of non-linear dynamics.

The analytical expressions for the non-linear normal modes, Eqs. (30) and (31), and non-linear multi-modes, Eqs. (54) and (55), have been developed for the beam with a distributed axial load by using the method of multiple scales. The solutions up to the third order have been retained and an invariant manifold has been constructed. This analytical treatment was to reduce the problem complexity and dimension; consequently to reduce the computational effort involved in further dynamical analyses.

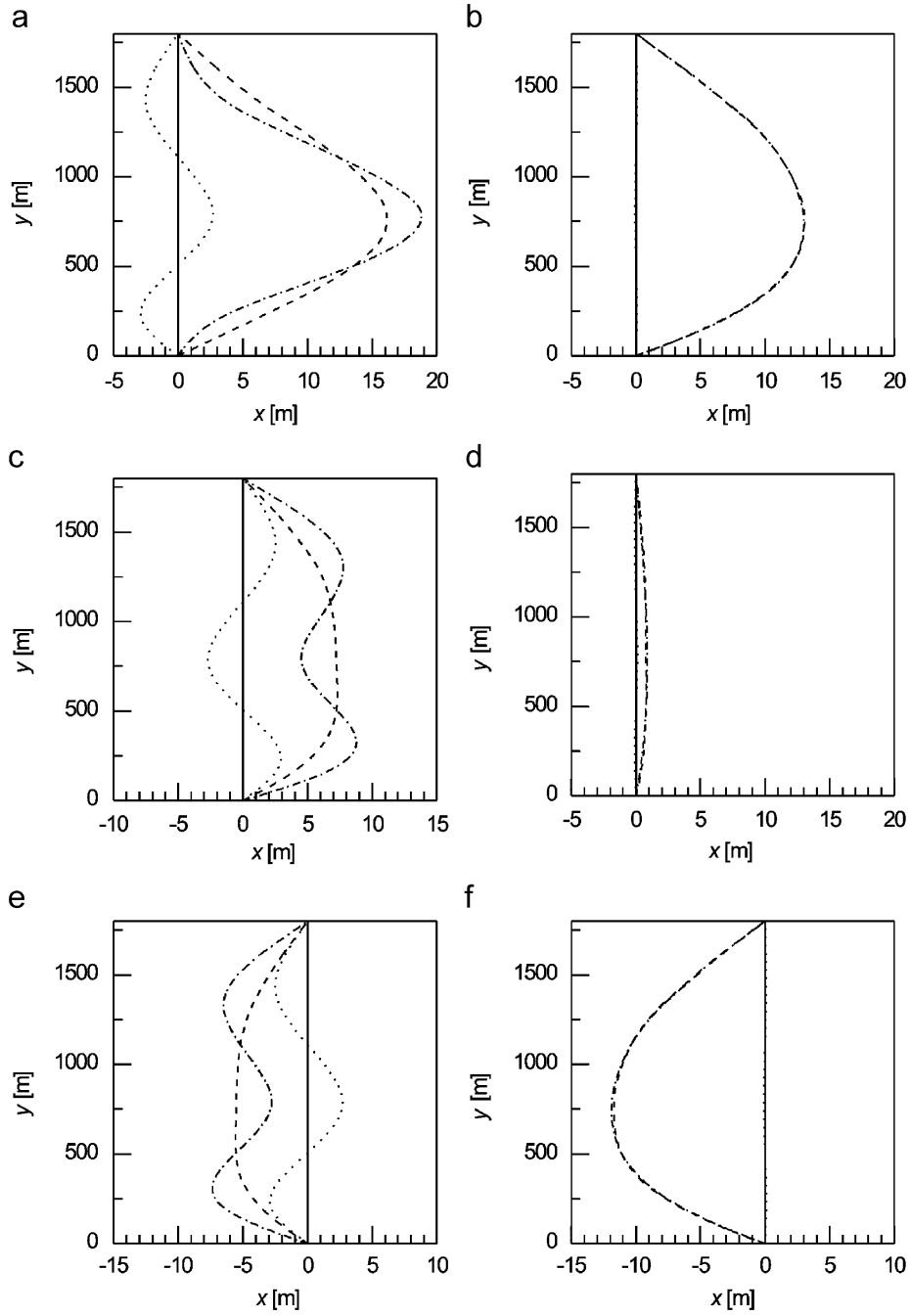

Fig. 7. Snapshots of the first and the third non-linear modes. Modal responses for: (a) $t=0.0$ s, (b) $t=3.1$ s, (c) $t=6.1$ s, (d) $t=9.2$ s, (e) $t=12.2$ s, and (f) $t=15.3$ s. Continuous line—reference configuration; broken line—NL mode 1; dotted line—NL mode 3; dash-dot line—multi-mode.

The developed analytical models have been verified against the results from FEM simulation undertaken on the FEM model of a vertical riser comprising 26 elements and having 77 DOF. The size of the model was dictated by a compromise between the accuracy and computational time, which on average took around 17 h on a fast PC. First, the dynamics at the mid-span was compared. The displacement magnitudes (Fig. 3) correspond well, but the phase portrait shapes and frequencies differ. The trajectory projections and phase portraits shown in Figs. 5 and 6 for the multi-modal responses correspond reasonably well. A further improvement in the analytical solution can be made by considering the normal force spatial variation. This is a topic of the authors' future studies.

Acknowledgements

The authors acknowledge a financial support from the Royal Society under a Joint Project scheme. The first author also acknowledges the support of CNPq under the Grant 304286/2003-6. The help with graphics by Dr. J. Wojewoda of TU Lodz is gratefully acknowledged. We are also thankful for valuable referees' comments.

Appendix A

Here it is assumed the non-linear axial strain, Eq. (3), to derive an equation of transversal motion for the considered slender beam.

The kinetic energy, neglecting rotational inertia, is

$$K = \int_0^\ell \frac{m}{2}(\dot{u}^2 + \dot{w}^2)\,\mathrm{d}x \tag{A.1}$$

from which, after taking into account the natural boundary conditions, it can be seen that

$$\int_{t_1}^{t_2} \delta K\,\mathrm{d}t = -\int_{t_1}^{t_2}\int_0^\ell m(\ddot{u}\delta u + \ddot{w}\delta w)\,\mathrm{d}x\,\mathrm{d}t. \tag{A.2}$$

As for the variation of the total potential energy, it is possible to write

$$\delta V = \delta U - \int_0^\ell p\delta u\,\mathrm{d}x + N_0\delta u_0, \tag{A.3}$$

where

$$\begin{aligned}\delta U &= \int_0^\ell \int_A E\varepsilon_P\delta\varepsilon_P\,\mathrm{d}A\,\mathrm{d}x \\ &= \int_0^\ell \int_A E\left(u' - zw'' + \frac{1}{2}w'^2\right) \\ &\quad\times(\delta u' - z\delta w'' + w'\delta w')\,\mathrm{d}A\,\mathrm{d}x.\end{aligned} \tag{A.4}$$

After integrating by parts it is found that

$$\begin{aligned}\delta U = &-\mathrm{EA}\varepsilon_0\delta u_0 - \int_0^\ell \mathrm{EA}(u'' + w'w'')\delta u\,\mathrm{d}x \\ &-\int_0^\ell \mathrm{EA}\left(u''w' + u'w'' + \frac{3}{2}w'^2w''\right)\delta w\,\mathrm{d}x \\ &+\int_0^\ell \mathrm{EI}\,w^{\mathrm{IV}}\delta w\,\mathrm{d}x,\end{aligned} \tag{A.5}$$

where ε_0 stands for the axis strain, Eq. (3), evaluated at $x=0$. Therefore

$$\begin{aligned}&\int_{t_1}^{t_2}\delta V\,\mathrm{d}t \\ &= (N_0 - \mathrm{EA}\varepsilon_0)\delta u_0 \\ &\quad-\int_{t_1}^{t_2}\int_0^\ell \mathrm{EA}\left(u'' + w'w'' + \frac{p}{\mathrm{EA}}\right)\delta u\,\mathrm{d}x\,\mathrm{d}t, \\ &\quad-\int_{t_1}^{t_2}\int_0^\ell \mathrm{EA}\left(u''w' + u'w'' + \frac{3}{2}w'^2w''\right)\delta w\,\mathrm{d}x\,\mathrm{d}t \\ &\quad+\int_{t_1}^{t_2}\int_0^\ell \mathrm{EI}\,w^{\mathrm{IV}}\delta w\,\mathrm{d}x\,\mathrm{d}t.\end{aligned} \tag{A.6}$$

The equations of motion are sought according to Hamilton's Principle:

$$\int_{t_1}^{t_2}(\delta K - \delta V)\,\mathrm{d}t = 0. \tag{A.7}$$

By substituting Eqs. (A.2) and (A.6) in Eq. (A.7), it is found that

$$\begin{aligned}&-(N_0 - \mathrm{EA}\,\varepsilon_0)\delta u_0 + \int_{t_1}^{t_2}\int_0^\ell\left[-m\ddot{u} + \mathrm{EA}\left(u''\right.\right. \\ &\quad\left.\left.+w'w'' + \frac{p}{\mathrm{EA}}\right)\right]\delta u\,\mathrm{d}x\,\mathrm{d}t, \\ &+\int_{t_1}^{t_2}\int_0^\ell\left[-m\ddot{w} + \mathrm{EA}\left(u''w' + u'w'' + \frac{3}{2}w'^2w''\right)\right. \\ &\quad\left.-\mathrm{EI}\,w^{\mathrm{IV}}\right]\delta w\,\mathrm{d}x\,\mathrm{d}t = 0, \quad \forall\delta u, \delta w.\end{aligned} \tag{A.8}$$

Since Eq. (A.8) must hold true for any virtual displacement, the following conclusions are drawn:

$$m\ddot{u} - \mathrm{EA}\left(u'' + w'w'' + \frac{p}{\mathrm{EA}}\right) = 0, \tag{A.9}$$

$$m\ddot{w} + \mathrm{EI}\,w^{\mathrm{IV}} - \mathrm{EA}[u'w'' + u''w' + \tfrac{3}{2}w'^2w''] = 0 \tag{A.10}$$

and

$$N_0 = \mathrm{EA}\,\varepsilon_0. \tag{A.11}$$

If inertial effects along the longitudinal direction are further neglected in Eq. (A.9)—see, for example Kauderer [21]—then

$$u'' + w'w'' + \frac{p}{\mathrm{EA}} = 0. \tag{A.12}$$

Integrating the above equation once with respect to x, one obtains

$$u' + \frac{1}{2}w'^2 + \frac{px}{\mathrm{EA}} = \varepsilon_0(t) \tag{A.13}$$

or simply,

$$\varepsilon(x,t) = u' + \frac{1}{2}w'^2 = \varepsilon_0(t) - \frac{px}{\mathrm{EA}}, \tag{A.14}$$

where $\varepsilon_0(t)$ can be evaluated by taking the average value on both sides of Eq. (A.13) along the beam length:

$$\varepsilon_0(t) = \frac{u_\ell - u_0}{\ell} + \frac{1}{2\ell}\int_0^\ell w'^2\,\mathrm{d}x + \frac{p\ell}{2\mathrm{EA}}. \tag{A.15}$$

Substituting from Eqs. (A.13) and (A.15) for u' and from Eq. (A.12) for u'' in Eq. (A.10), the following equation of transversal motion appears:

$$\begin{aligned}&m\ddot{w} + \mathrm{EI}\,w^{\mathrm{IV}} - \mathrm{EA}\left[\frac{u_\ell - u_0}{\ell} + \frac{1}{2\ell}\int_0^\ell w'^2\,\mathrm{d}x\right. \\ &\quad\left.+\frac{p}{\mathrm{EA}}\left(\frac{\ell}{2} - x\right)\right]w'' + pw' = 0.\end{aligned} \tag{A.16}$$

References

[1] C.H. Pak, R.M. Rosenberg, On the existence of normal mode vibrations in nonlinear systems, Q. Appl. Math. 26 (1968) 403–416.
[2] S.W. Shaw, C. Pierre, Non-linear normal modes and invariant manifolds, J. Sound Vib. 150 (1) (1991) 170–173.
[3] S.W. Shaw, C. Pierre, Normal modes for non-linear vibratory systems, J. Struct. 164 (1) (1993) 85–124.
[4] S.W. Shaw, C. Pierre, Normal-modes of vibration for nonlinear continuous systems, J. Sound Vib. 169 (3) (1994) 319–347.
[5] W. Lacarbonara, G. Rega, Resonant non-linear normal modes. Part I: activation/orthogonality conditions for shallow structural systems, Int. J. Non-linear Mech. 38 (2003) 873–887.
[6] O. Gendelman, L.I. Manevitch, A.F. Vakakis, L. Bergman, A degenerate bifurcation structure in the dynamics of coupled oscillators with essential stiffness nonlinearities, Nonlinear Dyn. 33 (1) (2003) 1–10.
[7] M.E. King, A.F. Vakakis, An energy-based approach to computing resonant nonlinear normal modes, J. Appl. Mech.—Trans. ASME 63 (3) (1996) 810–819.
[8] W. Lacarbonara, G. Rega, A.H. Nayfeh, Resonant non-linear normal modes. Part I: analytical treatment for structural one-dimensional systems, Int. J. Non-linear Mech. 38 (2003) 851–872.
[9] L.I. Manevitch, The description of localised normalised modes in a chain of nonlinear coupled oscillators using complex variables, Nonlinear Dyn. 25 (1–3) (2001) 95–109.
[10] L.I. Manevitch, O. Gendelman, A.I. Musienko, A.F. Vakakis, L. Bergman, Dynamic interaction of a semi-infinite linear chain of coupled oscillators with a strongly nonlinear end attachment, Physica D 178 (1–2) (2003) 1–18.
[11] Y.V. Mikhlin, Matching of local expansions in the theory of nonlinear vibrations, J. Sound Vib. 182 (4) (1995) 577–588.
[12] Y.V. Mikhlin, A.L. Zhupiev, An application of the Ince algebraization to the stability of non-linear normal vibration modes, Int. J. Non-Linear Mech. 32 (2) (1997) 393–409.
[13] Y.V. Mikhlin, B.I. Morgunov, Normal vibrations in near-conservative self-excited and viscoelastic nonlinear systems, Nonlinear Dyn. 25 (1–3) (2001) 33–48.
[14] A.F. Vakakis, R.H. Rand, Normal modes and global dynamics of a two-degree-of-freedom non-linear system—I. Low energies, Int. J. Non-Linear Mech. 27 (5) (1992) 861–874.
[15] A.F. Vakakis, R.H. Rand, Normal modes and global dynamics of a two-degree-of-freedom non-linear system—II. High energies, Int. J. Non-Linear Mech. 27 (5) (1992) 875–888.
[16] N. Srinil, G. Rega, S. Chucheepsakul, Two-to-one resonant multi-modal dynamics of horizontal/inclined cables. Part I: theoretical formulation and model validation, Nonlinear Dyn. 48 (2007) 231–252.

[17] N. Srinil, G. Rega, Two-to-one resonant multi-modal dynamics of horizontal/inclined cables. Part II: internal resonance activation, reduced-order models and nonlinear normal modes, Nonlinear Dyn. 48 (2007) 253–274.
[18] N. Srinil, G. Rega, The effects of kinematic condensation on internally resonant forced vibrations of shallow horizontal cables, Int. J. Non-Linear Mech. 42 (2007) 180–195.
[19] O.G.P. Baracho Neto, C.E.N. Mazzilli, Evaluation of non-linear normal modes for finite-element models, Comput. Struct. 80 (2002) 957–965.
[20] O.G.P. Baracho Neto, C.E.N. Mazzilli, Evaluation of multi-modes for finite-element models: systems tuned into 1:2 internal resonance, Int. J. Solids Struct. 42 (2005) 5795–5820.
[21] H. Kauderer, Nichtlineare Mechanik, Springer, Berlin, 1958.
[22] A.H. Nayfeh, S.A. Nayfeh, On nonlinear modes of continuous systems, J. Vib. Acoust. 116 (1994) 129–136.
[23] A.H. Nayfeh, C. Chin, S.A. Nayfeh, Nonlinear normal modes of a cantilever beam, J. Vib. Acoust. 117 (4) (1995) 477–481.
[24] G. Singh, A.K. Sharma, G.V. Rao, Large-amplitude free vibrations of beams—a discussion on various formulations and assumptions, J. Sound Vib. 142 (1) (1990) 77–85.
[25] S.W. Shaw, C. Pierre, E. Pesheck, Modal analysis-based reduced-order models for nonlinear structures—an invariant manifold approach, Shock Vib. Dig. 31 (1999) 3–16.
[26] C.T. Sanches, C.E.N. Mazzilli, L.D. Cunha, C.P. Pesce, Non-linear modal analysis applied to riser dynamics, in: Proceedings of the 17th International Offshore and Polar Engineering Conference, ISOPE'07, vol. 2, 2007, pp. 1–7.
[27] M.E.S. Soares, C.E.N. Mazzilli, Nonlinear normal modes of planar frames discretised by the finite element method, Comput. Struct. 77 (2000) 485–493.
[28] C.E.N. Mazzilli, M.E.S. Soares, O.G.P. Baracho Neto, Reduction of finite-element models of planar frames using non-linear normal modes, Int. J. Solids Struct. 38 (2001) 1993–2008.
[29] B.L. Newberry, N.C. Perkins, Analysis of resonant tangential response in submerged cables resulting from 1-to-1 internal resonance, in: Proceedings of the 7th International Offshore and Polar Engineering Conference, ISOPE'97, vol. II, Honolulu, 1997, pp. 157–163.
[30] C.P. Pesce, A.L.C. Fujarra, A.N. Simos, E.A. Tannuri, Analytical and closed form solutions for deep water riser-like eigenvalue problem, in: Proceedings of the 9th International Offshore and Polar Engineering Conference, ISOPE'99, vol. 2, 1999, pp. 255–264.
[31] C.P. Pesce, C.A. Martins, Numerical computation of riser dynamics, in: S. Chakrabarti (Ed.), Numerical Modelling in Fluid–Structure Interaction, Advances in Fluid Mechanics Series, WIT Press, Southampton, UK, 2005, pp. 253–309, (Chapter 7).
[32] C.P. Pesce, C.A. Martins, Riser-soil interaction: local dynamics at TDP and a discussion on the eigenvalue and the VIV problems, J. Offshore Mech. Arct. Eng. 128 (2006) 39–55.
[33] L.A. Pars, A Treatise on Analytical Dynamics, Heinemann, London, 1965.
[34] L. Meirovitch, Methods of Analytical Dynamics, McGraw-Hill, New York, 1970.
[35] A.H. Nayfeh, D.T. Mook, Nonlinear Oscillations, Wiley, New York, 1979.
[36] A.H. Nayfeh, Nonlinear interactions: analytical, computational and experimental methods, Meccanica 35 (6) (2000) 583–586.
[37] L.M.Y. Silveira, C.A. Martins, L.D. Cunha, C.P. Pesce, An investigation on the effect of tension variation on VIV of risers, in: Proceedings of OMAE, 2007, pp. 1–9.